An outer arm dynein light chain acts in a conformational switch for flagellar motility

Ramila S. Patel-King and Stephen M. King

Department of Molecular, Microbial, and Structural Biology, University of Connecticut Health Center, Farmington, CT 06030

A system distinct from the central pair–radial spoke complex was proposed to control outer arm dynein function in response to alterations in the mechanical state of the flagellum. In this study, we examine the role of a *Chlamydomonas reinhardtii* outer arm dynein light chain that associates with the motor domain of the γ heavy chain (HC). We demonstrate that expression of mutant forms of LC1 yield dominant-negative effects on swimming velocity, as the flagella continually beat out of phase and stall near or at the power/recovery stroke switchpoint. Furthermore, we observed that LC1 interacts directly with tubulin in a nucleotide-independent manner and tethers this motor unit to the A-tubule of the outer doublet microtubules within the axoneme. Therefore, this dynein HC is attached to the same microtubule by two sites: via both the N-terminal region and the motor domain. We propose that this γ HC–LC1–microtubule ternary complex functions as a conformational switch to control outer arm activity.

Introduction

To achieve a highly coordinated beat pattern, the dynein arms that power motile cilia and flagella must be tightly controlled so that waves of activity can propagate along the structure from base to tip. Previous studies have illustrated that multiple regulatory systems impinge upon these dynein motors. For example, in *Chlamydomonas reinhardtii*, these signals include those mediated through the central pair microtubules–radial spokes (for review see Smith and Yang, 2004) and dynein regulatory complex (Piperno et al., 1992) and involve responses to phosphorylation, Ca^{2+}, cAMP, and redox poise (Hyams and Borisy, 1978; Bessen et al., 1980; Hasegawa et al., 1987; Habermacher and Sale, 1997; King and Dutcher, 1997; Wakabayashi and King, 2006). Similar mechanisms have been identified in other organisms such as *Paramecium tetraurelia*, *Tetrahymena thermophila*, sea urchins, and mammals, indicating that these regulatory systems represent fundamental features of motile cilia/flagella (for review see Salathe, 2007). It is also clear from both theoretical models and experimental manipulation that dynein function responds to alteration in flagellar curvature and that this allows for propagation of motor activity along the axonemal length by sequential activation of motors (Sugino and Naitoh, 1982; Hayashibe et al., 1997; Lindemann, 2002; Brokaw, 2008; Hayashi and Shingyogi, 2008). Indeed, mechanical activation experiments in various *C. reinhardtii* mutants have suggested the presence of two mechanosensory systems: one involving the central pair microtubule complex and inner dynein arms, and a second separate system controlling outer arm function (Hayashibe et al., 1997).

The *C. reinhardtii* outer dynein arm has three distinct heavy chains (HCs; α, β, and γ) that each contain a unique N-terminal region involved in assembly and a C-terminal motor unit consisting of six AAA^+ domains, an ∼10-nm coiled-coil segment with a microtubule-binding site at its tip, and a C-terminal region of ∼40 kD. These motors are associated with two WD repeat intermediate chains (ICs) and 11 distinct light chain (LC) components (for review of *C. reinhardtii* dynein structure and organization see King and Kamiya, 2008). In addition, the trimeric docking complex (Takada and Kamiya, 1994), the Oda5p/adenylate kinase assembly (Wirschell et al., 2004), and Oda7p (Freshour et al., 2007), a putative inner arm–outer arm linker, are needed for assembly of this structure, as are several other gene products that have yet to be characterized. Furthermore, CrLis1, the *C. reinhardtii* orthologue of the lissencephaly protein Lis1, which acts as a cytoplasmic dynein regulatory component in mammals, also interacts with this motor (Pedersen et al., 2007) in a controlled manner (Rompolas, P., and S.M.

Correspondence to Stephen M. King: king@neuron.uchc.edu

Abbreviations used in this paper: EDC, 1-ethyl-3-(3-dimethylaminopropyl)carbodiimide; HC, heavy chain; IC, intermediate chain; LC, light chain; LRR, leucine-rich repeat; NMR, nuclear magnetic resonance.

The Rockefeller University Press $30.00
J. Cell Biol. Vol. 186 No. 2 283–295
www.jcb.org/cgi/doi/10.1083/jcb.200905083

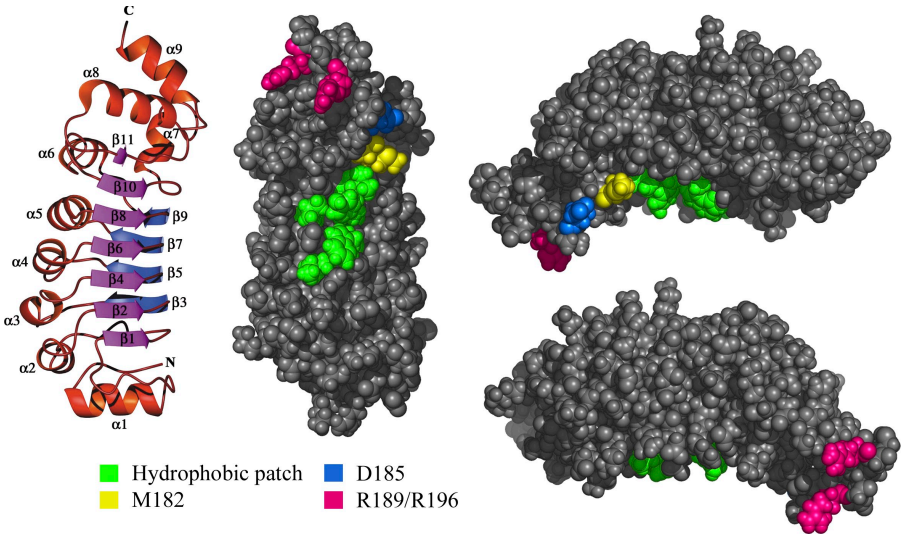

Figure 1. **Structure-based design of LC1 Mutants.** The mean LC1 ribbon structure (Protein Data Bank accession no. 1M9L; left) and three views of the van der Waals molecular surface (right) are shown. The LRR region forms two β sheets and a helical face. The larger β sheet face (left, magenta) contains a single hydrophobic patch (green) centered on W99 that is predicted to bind the γ HC. The C-terminal portion of LC1 consists of a helical region, the orientation of which is controlled by two residues (M182 [yellow] and D185 [blue]) that show high backbone dynamics. The terminal α9 helix likely protrudes into the AAA+ domain and contains two Arg residues (R189 and R196; pink) that potentially make ionic contacts with the motor domain and/or nucleotide.

King. 2008. American Society for Cell Biology Annual Meeting. Abstr. 275)

The outer arm is necessary to maintain normal flagellar beat frequency, as mutants that lack this structure show a significant reduction from 50–60 to ∼20 Hz with a consequent decrease in swimming velocity (Kamiya and Okamoto, 1985; Mitchell and Rosenbaum, 1985). In the absence of this motor, the photophobic or shock response, an alteration in waveform and swimming direction, which occurs in response to an increase in intraflagellar Ca^{2+} from *p*Ca 6 to *p*Ca 4 (Bessen et al., 1980), is defective (Kamiya and Okamoto, 1985; Mitchell and Rosenbaum, 1985); this appears to be mediated through the γ HC–associated calmodulin-related LC4 protein (Sakato and King, 2003; Sakato et al., 2007).

The γ HC is also associated with two copies of the leucine-rich repeat (LRR) protein LC1 (Pfister et al., 1982; Benashski et al., 1999) that interact with the motor domain; one copy is bound to AAA1 and the other is apparently bound to AAA3 or AAA4 (Benashski et al., 1999). This is the only integral axonemal dynein component known to interact directly with a motor unit. No mutants defective for LC1 are currently available. Therefore, to assess LC1 function, we have expressed a series of altered forms designed based on our nuclear magnetic resonance (NMR) structural and backbone dynamics analyses (Wu et al., 2000, 2003) in a wild-type background and show in this study that they exert a dominant-negative effect on flagellar motility. Furthermore, our biochemical data indicate that LC1 interacts directly with tubulin to form a γ HC–LC1–microtubule ternary complex. Thus, the γ HC N-terminal region and the motor domain both interact with the A-tubule of the same outer doublet. We suggest that LC1 acts as part of a conformational switch that controls outer arm dynein motor function during the flagellar beat cycle.

Results

Structure-based design of mutant forms of LC1

LC1 consists of an N-terminal helix capping a ββα barrel and a C-terminal helical region that protrudes from the main protein axis (Fig. 1; Wu et al., 1999, 2000, 2003). The hydrophobic patch (Fig. 1, colored green on the molecular surface) centered on W99 within the large β sheet is thought to mediate association with the γ HC, as this interaction is stable to high salt (Wu et al., 2000). Consequently, we predicted that the C-terminal α9 helix likely protrudes into the HC AAA+ domains. Previously, we demonstrated that two residues, M182 (Fig. 1, yellow) and D185 (Fig. 1, blue), exhibit high backbone dynamics (Wu et al., 2003) and may control the orientation of this helix. Furthermore, the α9 helix contains two Arg residues (R189 and R196; Fig. 1, pink) that potentially make ionic contacts within the AAA+ domains or with bound nucleotides (Wu et al., 2000, 2003); these latter residues were targeted, as, unlike the α and β HCs, the γ HC exhibits maximal ATPase activity at pH 10.0, suggesting that the ionization state of a basic residue is important in the catalytic and/or regulatory mechanism (Gatti et al., 1991).

To test the role of M182 and D185, we generated mutants in which these residues were altered to Gly or Pro in an effort to enhance or reduce flexibility, respectively; M182 was also altered to Ala. We also mutated R189 and R196 to either Ala or Asp/Glu to disrupt any ionic interactions mediated by these basic residues. Attempts to remove the entire α9 helix by truncating LC1 at either M182 or D185 were unsuccessful, as no mutant proteins were ever observed within the flagellum, although we did obtain many transformants containing the altered genes.

Mutagenesis and molecular analysis of transformed strains

To differentiate between endogenous and mutant forms of LC1, we inserted the 10-residue myc epitope tag near the N terminus after A2 (Fig. 2 a). This adds ∼1 kD of mass to the encoded protein and allows the wild-type and tagged copies to be readily differentiated after gel electrophoresis. The myc-tagged genes were introduced into the parental strain by transformation, and their insertion into the genome was confirmed by Southern blot analysis (Fig. 2 b). The endogenous LC1 gene yields a single ∼4.5-kb band after SmaI digestion of genomic DNA, and transformants contained additional bands, indicating incorporation of ≥1 copies of the tagged gene. As gene insertion in *C. reinhardtii* occurs essentially at random, not all additional gene copies are functional.

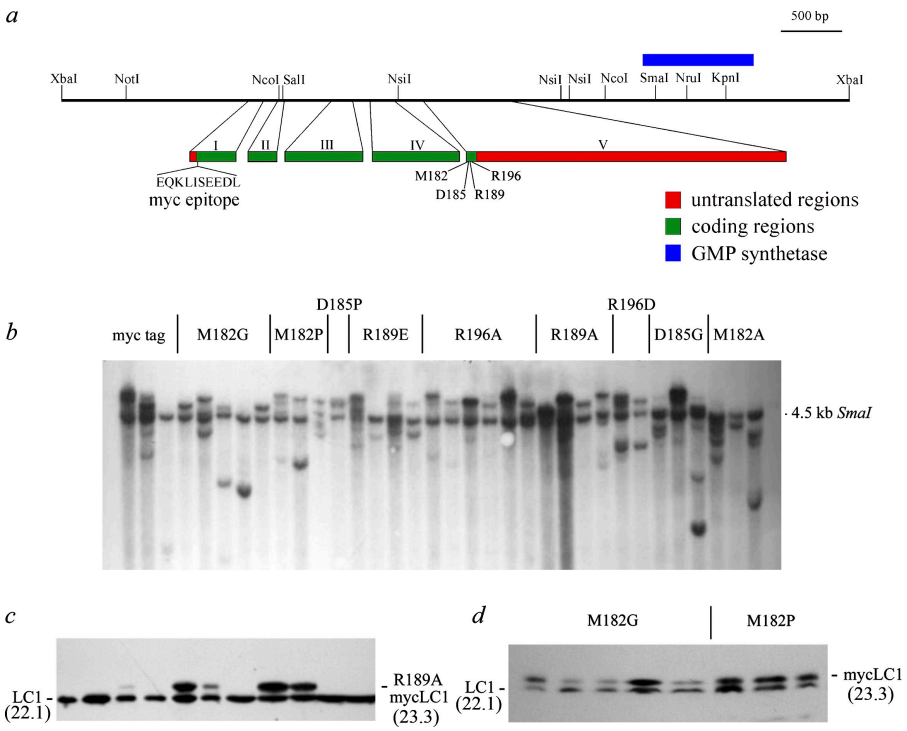

Figure 2. **Expression of tagged mutant versions of LC1.** (a) Map of the ~6.2-kb LC1 genomic region, indicating the location of the five exons and the sites of myc tag insertion and mutagenesis. The genomic fragment also includes the gene for GMP synthase. (b) Southern blot analysis of SmaI-digested genomic DNA from strains transformed with various mutant forms of LC1. The endogenous LC1 gene yields a SmaI fragment of ~4.5 kb (Benashski et al., 1999). The additional bands represent ≥1 integrated copies of the tagged LC1 gene. (c) Immunoblot analysis of flagellar samples from 11 strains transformed with the R189A mutant LC1 gene. The myc-tagged LC1 protein is detectable in five strains. (d) Immunoblot analysis of selected M182G- and M182P-transformed strains. These strains were chosen for analysis, as they stably express approximately similar amounts of wild-type and mutant LC1 proteins.

To identify strains that express tagged LC1 and incorporate the protein into the outer arm, samples of flagella were prepared from each transformant and probed with the R5932 antibody that specifically reacts with LC1 (Benashski et al., 1999). A representative immunoblot of flagella from cells transformed with the R189A mutant form of the LC1 gene is shown in Fig. 2 c. Wild-type LC1 migrates with M_r = 22,000, whereas the mutant-tagged protein forms a separate clearly distinguishable band. We routinely observed that 30–40% of transformants containing mutant genes actually expressed the tagged protein. Furthermore, in most cases, the relative amounts of wild-type and myc-tagged proteins present in the flagellum were similar; these strains were selected for further analysis (Fig. 2 d). We found that transgene expression was stable and that the amount of tagged protein incorporated into the flagellum did not vary significantly over several months.

Biochemical fractionation of flagella containing tagged mutant LC1 revealed that all mutant proteins were stably incorporated into the axonemal superstructure and could be solubilized by treatment with 0.6 M NaCl in a manner similar to the wild-type protein (Fig. 3 a, top). A small amount of LC1 was also found in the detergent-solubilized membrane/matrix fraction. In the case of both M182G (not depicted) and D185G (Fig. 3 a, bottom) transformants, the amount of myc-tagged

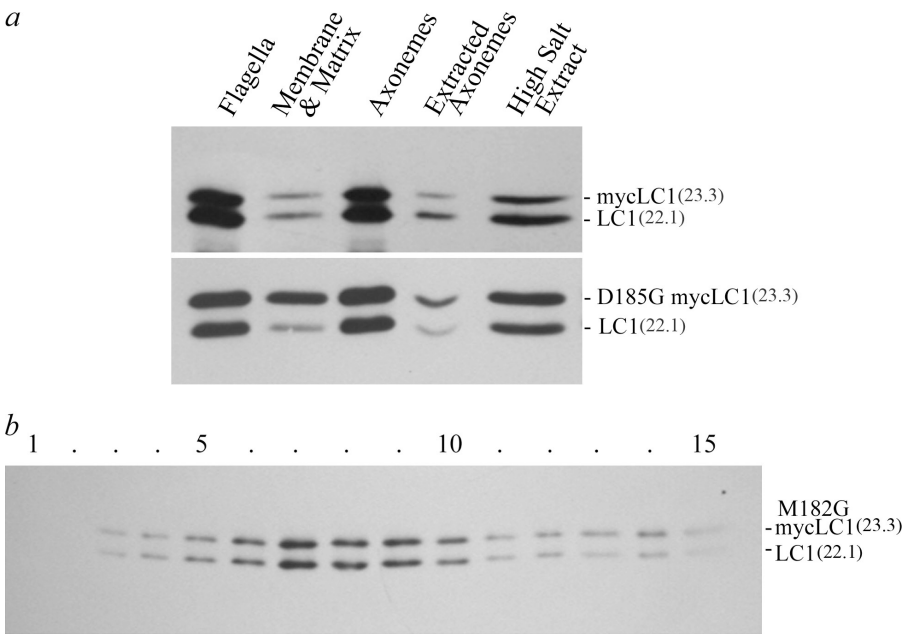

Figure 3. **Myc-tagged LC1 copurifies with the outer dynein arm.** (a) Immunoblots of flagellar fractions from strains expressing either myc-tagged LC1 or the D185G mutant form are shown. Addition of the myc tag alone (top) and most mutant forms did not alter either the detergent or 0.6 M NaCl extraction properties of LC1. In contrast, the D185G and M182G (not depicted) versions of LC1 exhibited an enhanced tendency to dissociate after detergent treatment of flagella (bottom). (b) Immunoblot of dynein from a strain expressing the M182G myc-tagged form of LC1 fractionated in a 5–20% sucrose density gradient; the bottom of the gradient is at left. The altered version of LC1 precisely comigrates with the native protein. Numbers in parentheses are given in kD.

Table I. **Motility defects caused by mutant LC1 proteins**

Strain/mutation	Swimming velocity[a]	Beat frequency[b]	Distance traveled/beat[c]	No. independent transformants analyzed	Axonemal ATPase activity
	μm/s	*Hz*	*μm*		*nmol phosphate released/min/μg protein*
WT (cc124)	129.9 ± 15.1	50–60	2.60	NA	0.18
cwd arg7-8 (cc3395)	115.1 ± 34.1	∼45	2.56	NA	ND
Myc tag	114.3 ± 15.8	45–50	2.54	9	0.17
M182A	81.8 ± 19.3	40–45	2.04	15	0.15
M182G	69.2 ± 18.1	40–45	1.73	13	0.18
M182P	55.7 ± 15.7	42–45	1.32	11	0.17
M182*[d]	ND	ND	ND	0	ND
D185G	31.5 ± 12.2	40–45	0.79	5	ND
D185P	38.2 ± 9.8	32–35	1.19	6	ND
D185*[d]	ND	ND	ND	0	ND
R189A[e]	64.5 ± 20.9	35–40	1.84	26	0.19
R189E	32.0 ± 15.1	35–40	0.91	14	0.17
R196A	45.6 ± 13.4	35–40	1.30	19	0.17
R196D	46.7 ± 10.2	30–40	1.55	7	ND

WT, wild type; NA, not applicable. Asterisks indicate stop codons.

[a]Determined from the tracks of at least 10 cells. Tracks were plotted in Metamorph, and statistical data were calculated from xy coordinates using Cell Motility Suite. Values are given as mean ± SD.

[b]Beat frequency was determined using the population-based fast Fourier transform method of Kamiya (2000). Each transformant was analyzed at least three times, and the range of peak values is reported.

[c]Determined from the mean swimming velocity and lower limit of the beat frequency data.

[d]We have not detected any transformants that incorporate LC1 truncated at either M182 or D185 into the flagellum.

[e]Several R189A transformants exhibited a markedly lower swimming velocity of 38.0 ± 28.8 μm/s and also had highly convoluted cell tracks.

mutant protein in this detergent-soluble fraction was enhanced over wild type. In contrast, all other LC1 mutants did not show significant differences in extraction properties. As both M182 and D185 show high dynamics, this increased detergent solubility is not caused by alteration in charge but more likely derives from enhanced flexibility of the terminal helix as a result of Gly insertion in the residues important for its orientation. After high salt extraction from the axoneme, dynein incorporating myc-tagged LC1 was fractionated in a 5–20% sucrose density gradient; the tagged versions of LC1 precisely cofractionated with the wild-type protein (Fig. 3 b). Attempts to assess whether tagged LC1 preferentially associates with one or other of the two binding sites on the γ HC were unsuccessful, as the myc epitope is not accessible within the native complex, and its immunoreactivity is destroyed by treatment with dimethyl pimelimidate, which is required to cross-link LC1 to the HC.

Phenotypic analysis of defects caused by LC1 mutations

We initially examined the flagellar beat frequency of multiple transformants and measured the swimming velocity and tracks of representative strains (Table I and Fig. 4). The *cwd arg7-8* strain used as the parental background for all transformations swam slightly more slowly than the cc124 wild-type strain (115 vs. ∼130 μm/s) and under our growth conditions had a beat frequency of ∼45 Hz compared with the wild-type 50–60 Hz. However, the distance traveled by *cwd arg7-8* cells per beat cycle was very close to the wild-type value (Table I). Insertion of additional *LC1* genes and expression of the myc-tagged form of the protein in *cwd arg7-8* had essentially no effect on swimming velocity or beat frequency (Table I). In contrast, we consistently observed significant and differential negative effects on swimming velocity when the LC1 C-terminal region was altered (Table I). Mutation of M182 to Ala was least disruptive, whereas alterations designed to enhance (M182G and D185G) or reduce (M182P and D185P) flexibility of the α9 helix yielded even slower velocities. Similarly, mutation of the Arg residues (R189 and R196) in helix α9 also resulted in significant phenotypes with velocities reduced to ∼25–50% of that of wild type. Although most strains had a beat frequency that was little different from the parental strain expressing myc-tagged LC1, the D185P mutation caused significant reduction to ∼32 Hz. We also found that several R189A transformants exhibited highly convoluted cell tracks (Fig. 4 b). Using the motility data to calculate the distance traveled per flagellar beat, we find that many of the strains expressing mutant LC1 proteins were propelled <50% of the wild-type distance per beat cycle (Table I). After dark adaption, strains expressing various myc-tagged forms of LC1 were able to perform the photoshock response upon illumination with bright white light and exhibited apparently normal phototactic behavior.

The outer arm contributes most (∼90%) of the ATPase activity of intact axonemes (Kagami and Kamiya, 1990), and lack of a single HC results in readily identified alterations in enzymatic function (Liu et al., 2008). Analysis of the axonemal ATPase activity of representative strains expressing mutant LC1 proteins (Table I) did not reveal any significant differences from wild type, which is consistent with the approximately normal beat frequencies observed in living cells.

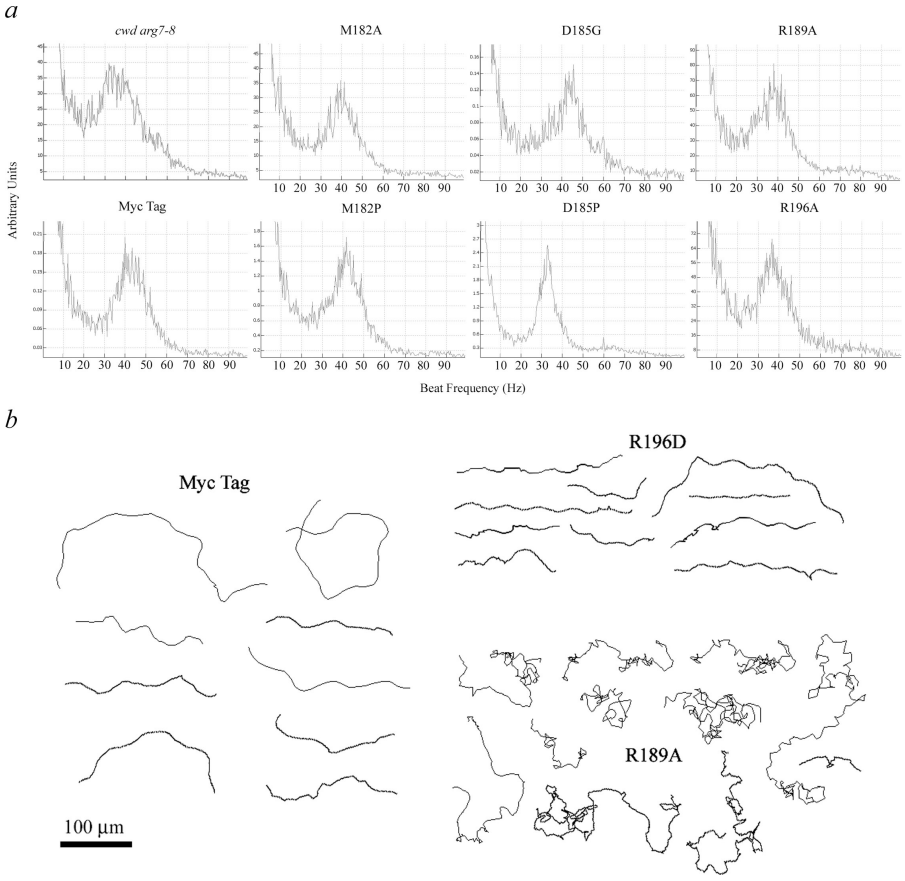

Figure 4. **Motile behavior of transformed strains.** (a) The beat frequency power spectra for the *cwd arg7-8* parental strain and transformants expressing myc-tagged LC1 and the M182A, M182P, D185G, D185P, R189A, and R196A mutant forms are shown. Strains incorporating the myc tag alone or the M182A, M182P, and D185G mutant forms have a beat frequency of ~40–45, Hz which is similar to the parental strain. Both R189A and R196A mutants had beat frequencies reduced somewhat to 35–40 Hz, and only D185P exhibited a more serious reduction to ~32 Hz. (b) The paths taken by individual cells expressing myc-tagged LC1 and the R196D and R189A mutant forms were tracked using MetaMorph. Most mutant strains moved in a helical path with occasional alterations in swimming direction as do wild-type cells. However, several R189A transformants swam very slowly and exhibited highly convoluted tracks as they continually altered direction.

To further assess the effects of LC1 mutations, we determined the propulsive force generated by the flagella of individual strains under varying viscous load conditions imposed by increased concentrations of Ficoll. As described previously by Yagi et al. (2005), we found that wild-type cells exhibited an ability to generate increased propulsive force as viscosity increased to ~2 cP (centipoise) before the value returned close to that obtained in buffer alone at higher viscosities; this response was completely absent from a strain (*oda6*) lacking outer dynein arms and was only barely detectable in the absence of the outer arm β HC motor unit (*oda4-s7*) (Fig. 5, top). In contrast, for a strain lacking the γ HC motor unit and LC1 (*oda2-t*), the amount of force generated at low viscosity approximated that observed in the complete absence of outer arms but more than doubled as viscosity was increased. This phenotype, due to the lack of the γ HC motor unit and/or LC1, was very similar to that observed for strains expressing M182G, R196A, and R189E mutant forms of LC1 (Fig. 5, bottom).

To determine why these strains exhibit low propulsive force and swimming velocity but do not have significant decreases in flagellar beat frequency, we examined the movement of individual cells under differential interference contrast optics using a high speed camera imaging at 600 frames per second. The flagella of wild-type cells exhibited well-coordinated power and recovery strokes (Fig. 6, top). In strains expressing the M182G (and also R189E and R196A; not depicted) versions of LC1, the two flagella continually beat completely out of phase with each other such that nearly all cells underwent large sideways rolling oscillations of up to ~50° as they moved forward (Fig. 6). Although this behavior is occasionally seen in wild-type cells, it is normally a transient response that returns to in-phase beating within a few beat cycles. In contrast, flagella of the LC1 mutant strains were almost always completely out of phase and were rarely observed to beat in a coordinated manner. Furthermore, superimposition of flagellar location during the beat cycle revealed a significant abnormality in the waveform (Fig. 6, diagram) such that the flagellum essentially stalled for a few milliseconds toward the end of the effective stroke before continuing the cycle. Thus, the flagella of strains expressing altered LC1 proteins are apparently defective in the conformational switching necessary to initiate the recovery stroke.

LC1 interacts directly with tubulin in situ

Previous zero-length cross-linking experiments (Benashski et al., 1999; Wu et al., 2000) revealed that LC1 is in direct contact with a protein of ~45 kD within the axoneme. However, this product was not generated after dynein extraction with 0.6 M NaCl, suggesting that p45 is not an integral component of the isolated dynein particle. We have been unable to purify this cross-linked product directly using biochemical methods. Therefore, to identify p45, we first incubated a nitrocellulose blot containing fractionated axonemal components with recombinant LC1 and then probed with the R5932 antibody (Fig. 7 a). We consistently observed that the tubulin band was bound by LC1. To further test whether p45 might be tubulin, recombinant LC1 was incubated in the presence or absence of taxol-stabilized

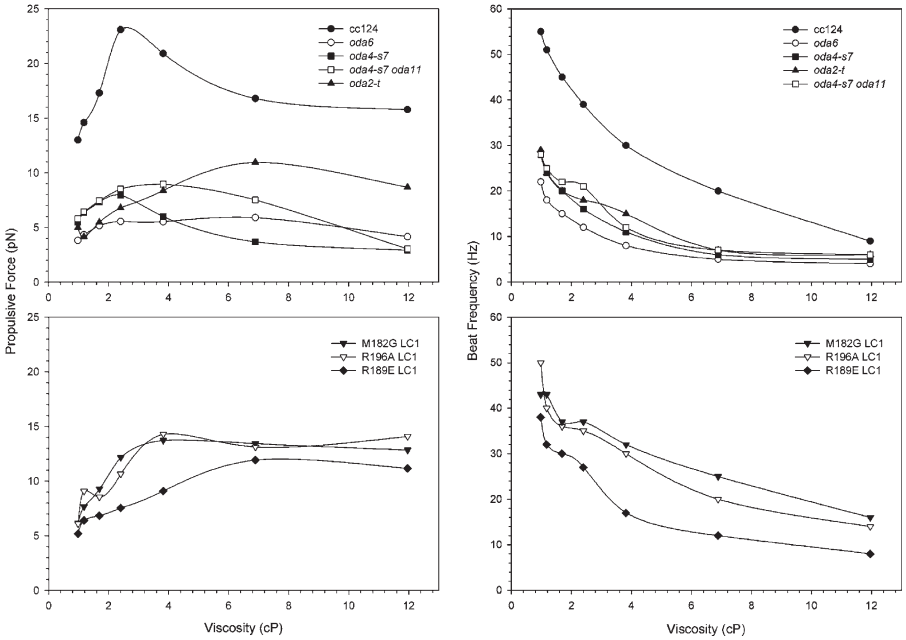

Figure 5. **Mutation of LC1 alters flagellar propulsive force generated under varying viscous load.** (top) The beat frequency and propulsive force generated under varying viscous load is shown for wild type (cc124) and for strains lacking the entire outer arm (*oda6*), the motor domains of the β and γ HCs (*oda4-s7* and *oda2-t*), and for a strain lacking both the β HC motor unit and the entire α HC (*oda4-s7 oda11*). (bottom) Similar plots for three strains expressing M182G, R189E, and R196A mutant forms of LC1 are shown. All three mutants generated reduced propulsive force under low viscous load, but this was enhanced as the load increased. This response approximates the behavior of the *oda2-t* mutant. Each point represents the mean propulsive force calculated from the swimming velocity of 10 cells. Bars indicating the SDs have been omitted for clarity; for all but two points on the cc124 and M182G plots, SDs ranged from 0.45–2.94 pN. Beat frequency data were obtained using the population-based fast Fourier transform method, and each determination was performed in triplicate.

microtubules, and the sample was subsequently centrifuged using an airfuge. Electrophoretic analysis of the resulting supernatants and pellets revealed that considerable LC1 was present in the pellet only when microtubules were added (Fig. 7 b). Stoichiometry measurements based on Coomassie blue dye binding suggest an ∼1:1 ratio of LC1 to tubulin monomer. Furthermore, when axonemes were treated with 1-ethyl-3-(3-dimethylaminopropyl)carbodiimide (EDC) and probed with the B-5-1-2 monoclonal antibody raised against sea urchin α-tubulin, we observed the formation of tubulin dimers and two additional

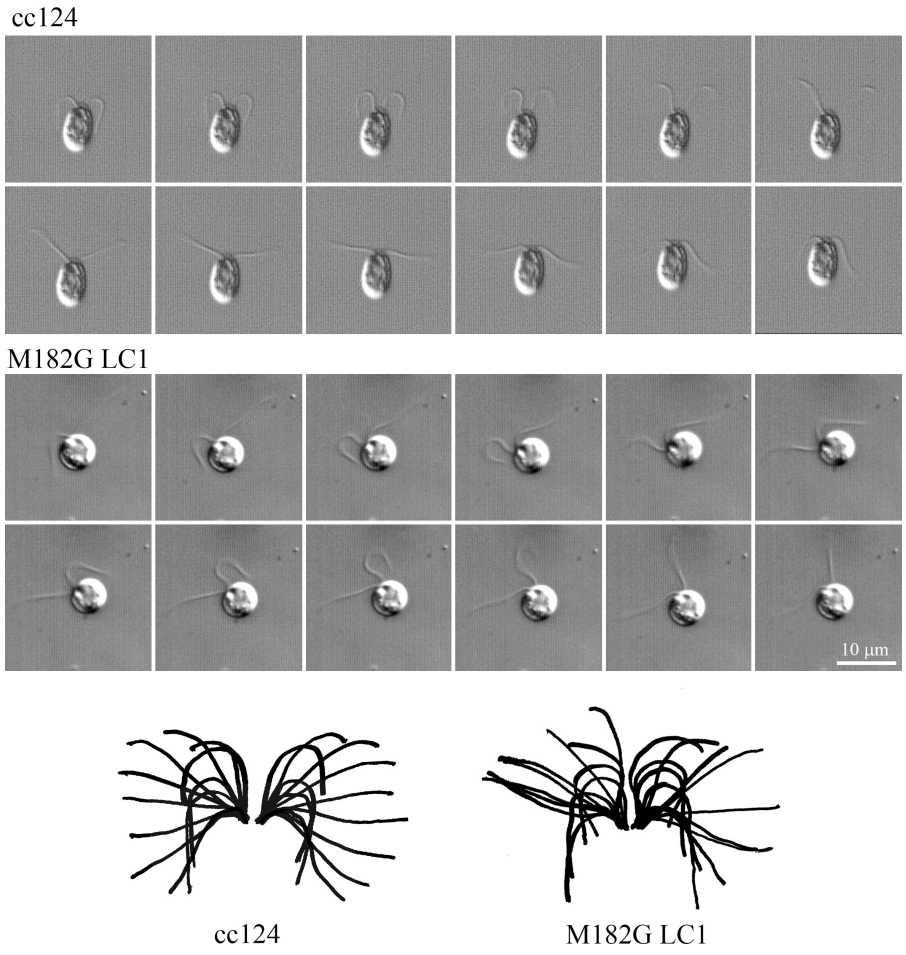

Figure 6. **Strains expressing mutant LC1 proteins exhibit alterations in flagellar phasing and the power/recovery stroke transition.** Montages of individual sequential frames (1.67 ms apart) from high speed recordings illustrating the waveform of the cc124 wild type and a strain expressing the M182G mutant form of LC1 are shown. Flagellar of the mutant strain continually beat completely out of phase, leading to a rolling motion of the cell body of ∼50° in the plane of the flagella during the beat cycle. (bottom) Diagrams illustrating the superimposed waveforms are shown. Flagella containing mutant LC1 essentially stall for several milliseconds toward the end of the effective stroke, suggesting that they are inefficient at initiating the recovery stroke.

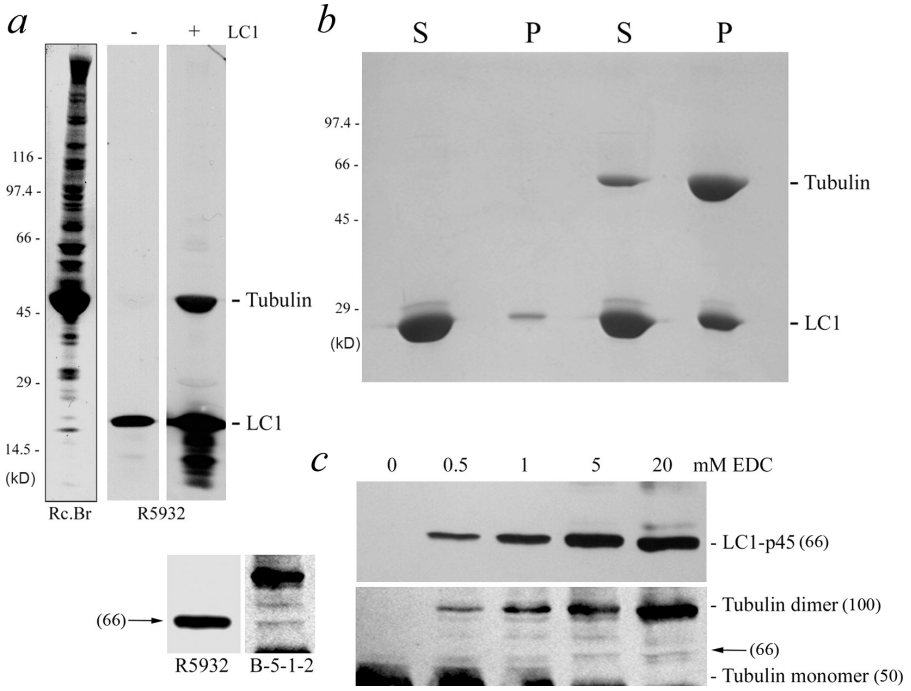

Figure 7. **Association of LC1 and tubulin within the axoneme.** (a) Nitrocellulose blots of axonemal proteins separated in a 5–15% acrylamide gradient gel were incubated in the presence or absence of recombinant LC1 and probed with the R5932 antibody. In the presence of LC1, the tubulin band was recognized, suggesting that LC1 binds tubulin. (left) The blot stained with Reactive brown 10 to detect total protein is shown. (b) Recombinant LC1 was incubated in the presence or absence of taxol-stabilized microtubules and spun in an airfuge for 5 min. Samples were electrophoresed in a 10% acrylamide gel and stained with Coomassie blue. In the absence of microtubules, only a very small fraction of LC1 was found in the pellet. However, upon microtubule addition, considerable LC1 bound microtubules and was present in the pellet fraction. Densitometry based on Coomassie dye binding indicated that the pellet contained a tubulin monomer/LC1 ratio of 1.00:1.06. (c) Axonemes were treated with 0–20 mM EDC, separated in an 8% acrylamide gel, blotted to nitrocellulose, and probed with R5932 and B-5-1-2 antibodies to detect LC1 and α-tubulin, respectively; note that most of the tubulin monomer band was excised from the blot before immunoblotting, as it produces a massive signal that otherwise obscures minor bands. The B-5-1-2 antibody detected two minor tubulin-containing products migrating between the tubulin monomer and dimer bands. The lower of these products precisely comigrated with the LC1-p45 band and was generated with similar kinetics. Numbers in parentheses indicate the approximate molecular mass of the indicated bands (given in kD).

tubulin-containing cross-linked bands that migrated between the tubulin monomer and dimer bands. The smaller of these products precisely comigrated with the LC1-p45 band and was generated with similar kinetics (Fig. 7 c). Thus, we conclude that p45 is tubulin.

To test whether the myc epitope and/or mutations affect LC1–tubulin interactions, axonemal samples from representative strains were treated with 0 or 5 mM EDC, and the blots then probed to reveal either LC1 or the myc epitope (Fig. 8 a). Myc-tagged protein was readily incorporated into the M_r 66,000 LC1–tubulin band, and both myc-tagged and wild-type proteins reacted with similar kinetics, suggesting that these mutations do not dramatically alter the interaction of LC1 with tubulin. To further assess tubulin–LC1 interactions in situ, we treated isolated axonemes with the zero-length cross-linking reagent EDC in the absence of nucleotide and in the presence of 1 mM ATP, 1 mM ADP, 1 mM ATP plus 100 μM vanadate, and 100 μM vanadate alone. The M_r 66,000 LC1–tubulin cross-linked product was generated with similar yields under all conditions, suggesting that this interaction is stable and not modulated in a nucleotide-sensitive manner (Fig. 8 b). In addition to the M_r 66,000 band, several higher order products that show mass increases in steps of ~50 kD were obtained; these likely represent cross-linking of the M_r 66,000 complex to additional tubulin monomers.

Previously, we observed that the N-terminal domain of the γ HC undergoes a large conformational alteration after Ca^{2+} binding to the associated LC4 protein (Sakato et al., 2007). To test whether this affects the γ HC–LC1–tubulin ternary complex in situ, we incubated axonemes with EDC in the presence and absence of ATP/vanadate under either high Ca^{2+} conditions or in the presence of 1 mM EGTA (Fig. 8 c). We observed no significant differences in the yield of the LC1–tubulin cross-linked product, suggesting that LC1–microtubule interactions are not modulated in response to Ca^{2+}.

LC1 associates with the A-tubule of the outer doublet microtubules

In situ, LC1 might be associated with the A-tubule of the outer doublet to which the dynein arm is permanently attached or with the B-tubule of the adjacent doublet upon which the arm acts to generate force. Therefore, to determine whether γ HC–associated LC1 is bound to the A- or B-tubules of the axonemal outer doublets, we incubated axonemes from the *oda4-s7 oda11* double mutant (lacks the entire α HC and β HC motor domain) with the R5932 antibody followed by a goat anti–rabbit IgG secondary antibody conjugated to 5 nm colloidal gold. As the γ HC is the innermost motor of the outer arm, axonemes from the double mutant were used for these experiments, as lack of the α and β HC motors was predicted to allow enhanced access of the antibody to the internal portions of the axoneme. Representative images of an axoneme and individual doublet microtubules with associated gold particles are shown in Fig. 9. Gold particles were found to cluster near the A-tubule and the basal region of the outer arm. In contrast, when the primary antibody was excluded, no axoneme-associated gold particles were observed. These data strongly suggest that LC1 is associated with the outer doublet A-tubule. Therefore, the γ HC appears to be tethered to the same microtubule by two distinct mechanisms: the N-terminal region is bound via the IC–LC complex and the motor unit by LC1.

Discussion

In this study, we demonstrate that the LRR protein LC1 attaches the motor unit of the γ HC of *C. reinhardtii* outer arm dynein to the A-tubule of the outer doublet microtubules within the flagellum in

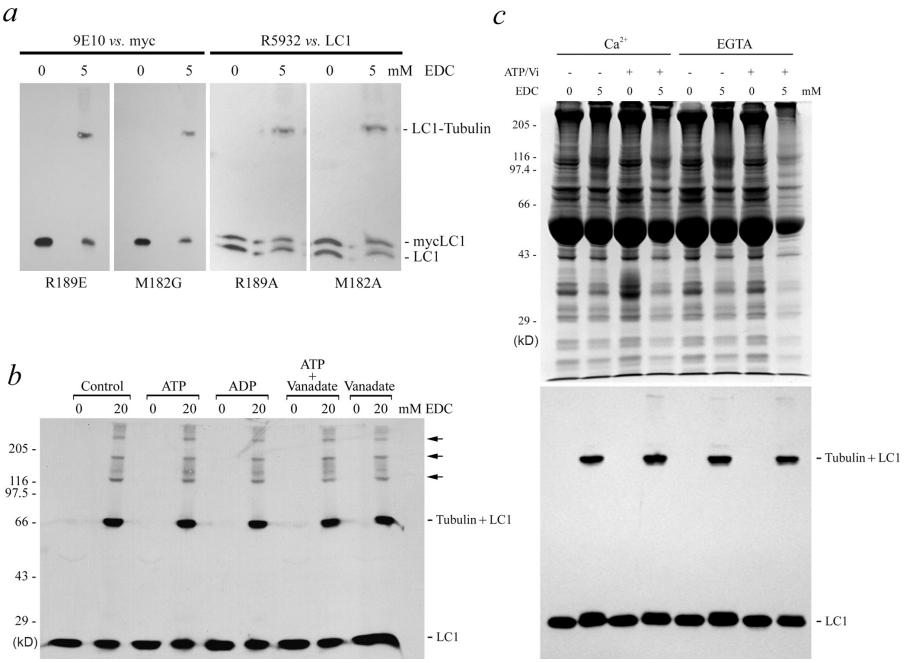

Figure 8. **Properties of LC1–tubulin interactions in situ.** (a) Axonemes from strains expressing mutant myc-tagged forms of LC1 were treated with 0 or 5 mM EDC electrophoresed and immunoblotted using the 9E10 monoclonal antibody against the myc epitope or R5932 to detect LC1. In all strains examined, myc-tagged LC1 was readily incorporated into the M_r 66,000 LC1–tubulin cross-linked product, indicating that these proteins remain in direct contact. Furthermore, there were no obvious differences in the rate of incorporation of the tagged mutant forms compared with wild type, as both LC1 and myc-LC1 bands were reduced with similar kinetics. (b) Axonemes were treated with either 0 or 20 mM EDC in buffer or in the presence of 1 mM ATP, 1 mM ADP, 1 mM ATP plus 100 µM vanadate, and 100 µM vanadate alone. Samples were electrophoresed in a 5–15% acrylamide gradient gel, blotted to nitrocellulose, and probed with the R5932 antibody. The M_r 66,000 LC1–tubulin cross-linked product was generated by EDC treatment in similar yield under all nucleotide conditions, suggesting that LC1 and tubulin are permanently tethered to each other during the mechanochemical cycle. Several of the higher order products (arrows) show mass increase in steps of ~50 kD and likely derive from cross-linking of the LC1–tubulin product to ≥1 additional tubulin molecules. (c) To test whether LC1–tubulin interactions were modified in a Ca^{2+}-dependent manner, axonemes were resuspended in buffer containing 1 mM Ca^{2+} or EGTA in the presence or absence of 1 mM ATP/100 µM vanadate and were subsequently treated with 0 or 5 mM EDC. Samples were electrophoresed in a 10% acrylamide gel and stained with Coomassie blue (top) or probed with the R5932 antibody against LC1 (bottom). No differences in the yield of the LC1–tubulin product were observed as a consequence of Ca^{2+} addition.

an ATP-independent manner. Furthermore, subtle alterations in LC1 lead to substantial decreases in swimming velocity as the result of a reduction in the propulsive force generated, which is caused by aphasic flagellar beating and by stalling of the flagella toward the end of the power stroke. These observations suggest that LC1 is essential for normal outer arm dynein motor function. Our data support a model in which this dynein motor is permanently tethered to the A-tubule of the outer doublet microtubule by two attachment sites and potentially acts as a conformational switch that alters dynein motor function in response to changes in flagellar curvature.

The LC1–γ HC complex as a conserved feature of outer arm dynein

Biochemical studies indicate that outer arm dyneins from unikonts (e.g., sea urchins and chordates; Bell et al., 1979; Belles-Isles et al., 1986; Gatti et al., 1989) have only two HCs, whereas those from bikonts (e.g., *C. reinhardtii* and *T. thermophila*; Pfister et al., 1982; Porter and Johnson, 1983) have three. However, phylogenetic analysis indicates that there is an underlying similarity in that both groups contain HCs that are the functional equivalents of the β and γ HCs of *C. reinhardtii*, with the additional HC in bikonts being a modified form of the β HC (Wickstead and Gull, 2007). Similarly, the γ HC–associated LC1 protein has been highly conserved and, for example, the mammalian and algal forms share 54% sequence identity. Even though purified outer arm dynein contains two ICs and 11 LCs in addition to the three HCs, LC1 is unusual in that it is the only component that binds directly to an HC motor unit rather than to either the N-terminal domain or the basal IC–LC complex (Benashski et al., 1999). Indeed, mapping studies (Benashski et al., 1999) indicate that one copy of LC1 associates with the AAA1 domain that hydrolyzes ATP and that a second copy binds the AAA3 or AAA4 domains that apparently act as allosteric regulators of motor function (Cho et al., 2008).

The RNAi knockdown of an LC1 homologue (TbLC1) in the excavate *Trypanosoma brucei* resulted in the partial disruption of outer arm assembly, misorientation of the central pair apparatus, and a reversal of swimming direction as the result of a change in waveform (Baron et al., 2007). This observation suggested that LC1 might be necessary for stable incorporation of the arm within the axonemal superstructure. The *C. reinhardtii oda2-t* mutant assembles outer dynein arms that completely lack both the γ HC motor unit and LC1 (Liu et al., 2008); thus, in this organism, LC1 is not required for assembly of outer arms containing truncated γ HCs. However, it remains possible that LC1 is required to stabilize the full-length γ HC in cytoplasm; if this is the case, lack of LC1 in *T. brucei* would lead to the absence of the γ HC, which would likely disrupt outer arm assembly.

The loss of a tip to base waveform observed in trypanosomes upon LC1 reduction may also reflect the lack of outer arm assembly, as the RNAi knockdown of a dynein IC in that organism resulted in a related phenotype, although in that case, the cells did not move backward (Branche et al., 2006). Further analysis of the *C. reinhardtii oda2-t* mutant revealed that the conserved γ HC–LC1 complex is necessary for wild-type motility, as the mutant cells swam at approximately half the velocity of wild type. Moreover, when *oda2-t* axonemes were reactivated under high Ca^{2+} conditions, only a low percentage actually beat, and those that did showed a symmetrical waveform of abnormally low amplitude that was ineffective for propulsion (Liu et al., 2008).

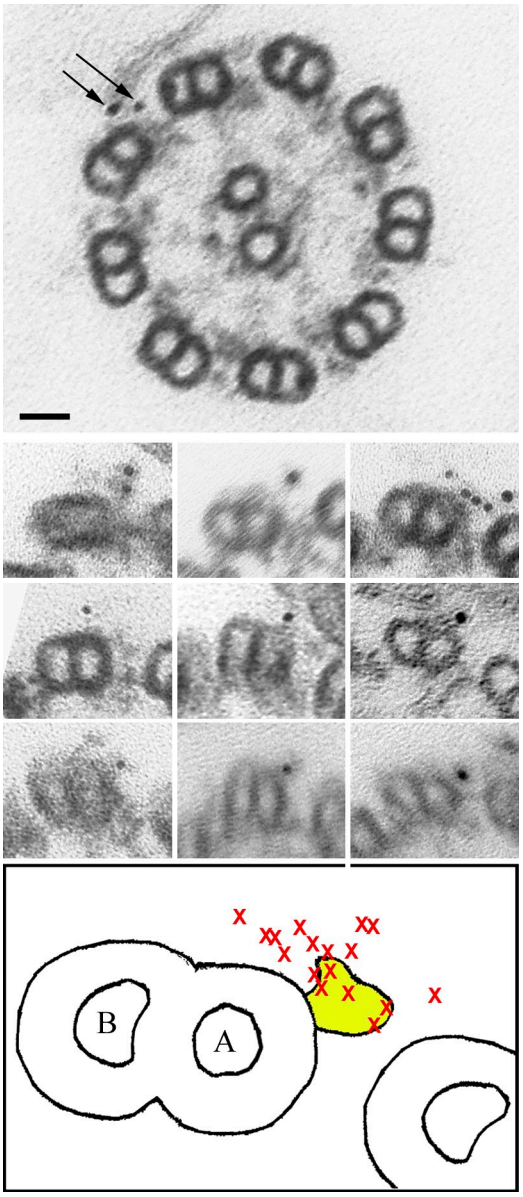

Figure 9. **Immunogold localization of LC1 within *oda4-s7 oda11* axonemes.** Electron micrographs of cross sections through an *oda4-s7 oda11* axoneme (top) and individual outer doublets (middle) that had been incubated with antibody against LC1 and a secondary antibody conjugated to 5 nm gold. (bottom) A diagram illustrating the outer arm from this strain (yellow) and the location of individual gold particles (marked by x) is shown. The gold particles are clustered near the A-tubule of the doublet to which the outer arm is permanently attached. Arrows indicate two individual gold particles. Bar, 25 nm.

Geometry of the γ HC–LC1–microtubule ternary complex

The largest axial dimension of LC1 is ∼70 Å (Fig. 10 a), and within the axoneme, there are two microtubules that γ HC–associated LC1 potentially could bind: the A-tubule of the microtubule doublet to which the outer arm is permanently attached and the B-tubule of the adjacent doublet upon which the outer arm acts to generate force (Fig. 10 b). Based on the cryo-EM reconstructions of outer arm–microtubule complexes (Oda et al., 2007), the γ HC motor unit is located ∼6 nm from the microtubule to which the IC–LC complex is bound and >10 nm from the adjacent microtubule (Fig. 10 c). This is consistent with tomographic reconstructions of *C. reinhardtii* axonemes, which indicate that the B-tubule is ∼12 nm distant from the AAA$^+$ ring of the γ HC motor unit (Nicastro et al., 2006; Ishikawa et al., 2007). Furthermore, the inter doublet distance increases by ∼10 nm in a bent region of the flagellum compared with a straight segment (Lindemann and Mitchell, 2007). Thus, given these spatial constraints and the axial dimensions of LC1 (Fig. 10 a), it is unlikely that this protein could span the gap to the B-tubule without a significant alteration in the location of the γ HC AAA$^+$ ring. In contrast, the geometry of the system is consistent with LC1 binding to the A-tubule. To test this directly, we localized LC1 in situ by immuno-EM and found that the gold particles were closely associated with the A-tubule near the outer arm attachment site.

Analysis of mutant axonemes lacking individual motors has indicated that the γ HC is the innermost HC within the outer arm (Sakakibara et al., 1993; Liu et al., 2008), and electron tomography revealed a continuity of density between the A-tubule of the outer doublet microtubules and the γ HC motor domain (Nicastro et al., 2006; Ishikawa et al., 2007). Similarly, a distinct connection between the γ HC AAA$^+$ ring and the microtubule to which dynein is permanently attached was observed in cross-bridged dynein–microtubule complexes (Fig. 10 c; Oda et al., 2007). These analyses are consistent with our suggestion that LC1 bridges the gap between the γ HC AAA$^+$ ring and the outer doublet A-tubule.

Motility defects caused by mutant forms of LC1

We found that strains expressing mutant versions of LC1 exhibited intriguing motility defects. First, these strains swam significantly more slowly than controls even though beat frequency was not drastically altered, resulting in an ∼50% reduction in the forward movement generated per beat. This implied that the waveform had been significantly altered to a pattern that was less capable of generating propulsive force. To directly test whether this was indeed the case, we determined the amount of propulsive force generated by these strains as well as mutants lacking various outer arm dynein components. The LC1 mutants exhibited a response to varying viscous load that was similar to that observed for the *oda2-t* mutant; this strain lacks both the γ HC motor unit and LC1. In buffer alone, these strains behaved as if they completely lacked the outer dynein arm, but the amount of propulsive force generated approached wild-type levels under high viscous load. These observations further implicate LC1 as a key component in γ HC function that becomes progressively less critical under increasingly high viscosity where beat frequency is significantly reduced. To directly assess the waveform, we imaged the flagellar beating of several mutant strains and found that they have two basic defects. Most obviously, the two flagella beat asynchronously and were rarely seen in phase. This resulted in a rolling forward motion such that a point at the flagellar base moved sideways by up to 50° during the beat cycle. The second defect was that the flagella exhibited an aberrant transition from the power stroke to the recovery stroke such that they essentially stalled for several milliseconds.

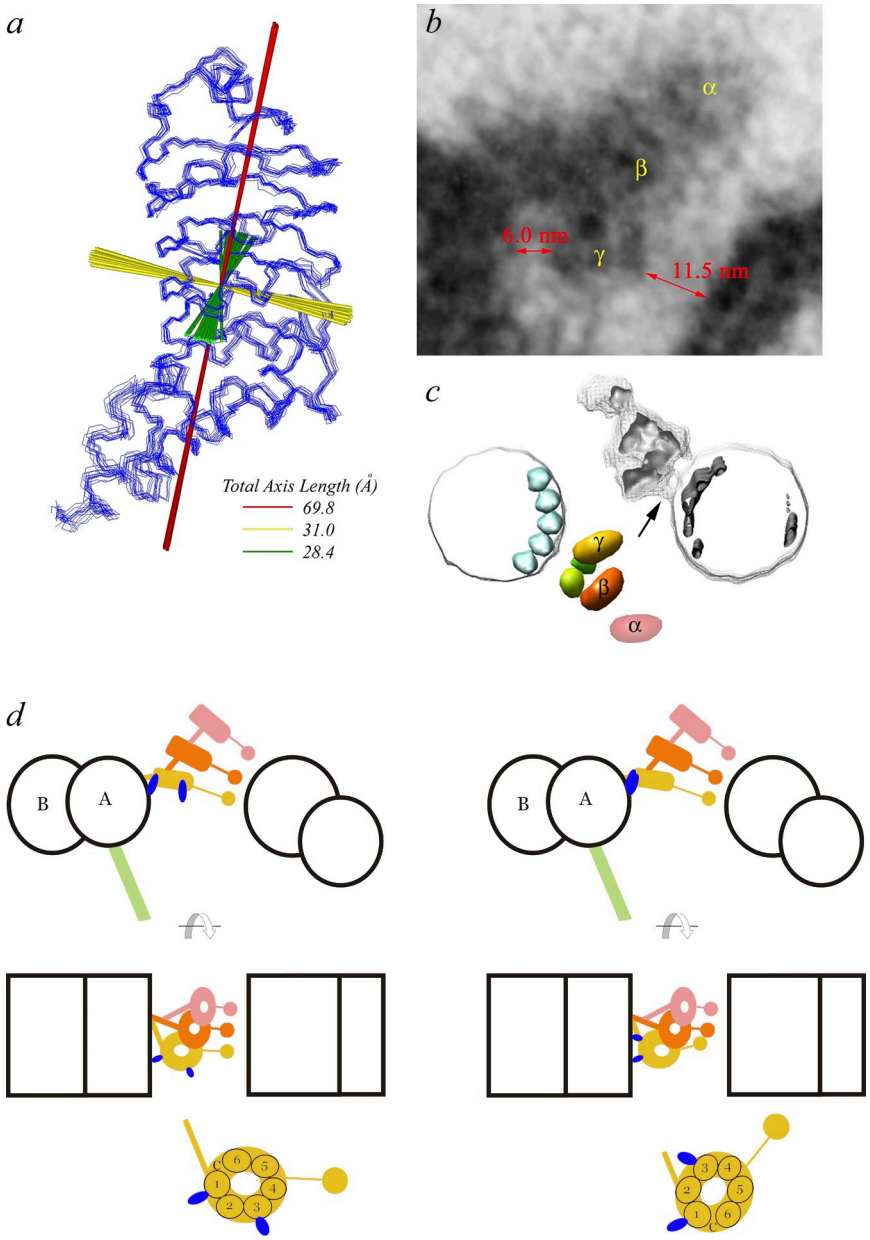

Figure 10. **Geometry of the γ HC–LC1–microtubule ternary complex in situ.** (a) The principal molecular axes of LC1 are superimposed on the ensemble of NMR-derived backbone structures (Protein Data Bank accession no. 1M9L) and the total axial dimensions indicated. LC1 is highly asymmetric with an axial ratio of 1.00 (green):1.13 (yellow):2.46 (red). (b) Thin section electron micrograph of the outer dynein arm in situ. The regions occupied by the motor domains of the three HCs are indicated as are the approximate distances between the γ HC motor unit and the neighboring outer doublet microtubules. (c) Three-dimensional reconstruction of the outer dynein arm–microtubule rigor complex from cryo-EM tomograms. Pink, α HC; orange, β HC; yellow, γ HC. There is a clear connection (arrow) between the γ HC motor unit and the microtubule to which the dynein is bound. The reconstruction is modified from Oda et al. (2007). (d) Models illustrating two potential geometries for the γ HC–LC1–microtubule complex in which LC1 is proposed to tether the γ HC to the A-tubule of the doublet to which dynein is permanently attached via the IC–LC complex and the docking complex. The HC color scheme is the same as in c. These models are based on the known dimensions of LC1, the measured motor unit/microtubule distances, and the immunogold localization of LC1 to the A-tubule. (left) The γ HC motor unit is in the same orientation as those of the α and β HCs. In this situation, it is unlikely that both copies of LC1 could interact simultaneously with the A-tubule. Thus, it is possible that the copy of LC1 that is bound switches as the AAA motor unit alters conformation during the mechanochemical cycle. (right) The γ HC motor unit is oriented differently such that both copies of LC1 bind the A-tubule simultaneously. In this situation, the system may act as a brake to limit sliding rather than as a microtubule translocase.

This suggests that a functional LC1–γ HC complex is required for outer arm dynein control during this transition and is consistent with the model presented by Hayashibe et al. (1997), which invoked a separate mechanosensory system for outer arm control distinct from the one emanating from the central pair microtubule complex that impinges on the inner arms. Intriguingly, an out of phase ("hands up, hands down") orientation was also observed for the arrested flagella of cells treated with an RNAi construct to reduce expression of hydin, which has been suggested to participate in conformational switching mediated by the central pair complex and radial spokes (Lechtreck and Witman, 2007).

One possible reason for the out of phase beating is that coordination between the cis- and trans-flagellum, which have inherently different intrinsic beat frequencies, has been disrupted. However, although this property is mediated through the outer arm, it appears to involve the α HC (Sakakibara et al., 1991) and docking complex (Takada and Kamiya, 1997). Thus, it seems more likely that out of phase beating in the mutant LC1-expressing strains results from the flagella stalling for random periods toward the end of the power stroke. In addition, these observations also provide an explanation for the varying reductions in swimming velocity caused by the different mutations, as they may result in subtle differential effects on the stall time at the end of the power stroke and/or on the frequency with which the two flagella are able to beat in phase.

Implications for dynein motor function

It is feasible that LC1 merely acts as a tether to attach the motor unit to the outer doublet A-tubule. However, although the various point mutations caused dramatic motility defects, we did not detect any major alteration in either LC1–γ HC or LC1–tubulin interactions. Rather, our data suggest that LC1 not only tethers the motor unit but also actively controls γ HC function and that defects lead to stalling at the conformational switch point between power and recovery strokes.

Electron microscopic analysis of inner arm dynein c under various nucleotide conditions led to a model in which the dynein motor unit rotates with respect to the N-terminal stem during the power stroke (Burgess et al., 2003). This model received further support from fluorescence resonance energy transfer measurements of cytoplasmic dynein motor units labeled with two fluorophores (Kon et al., 2005) and from experiments that located individual domains in the apo and ADP-vanadate forms of the enzyme (Roberts et al., 2009). Experiments aimed at defining the consequences of alterations in the register of the coiled-coil domain that terminates in the microtubule-binding site (Carter et al., 2008) led to an alternative model whereby the AAA^+ motor unit ring remains in a constant orientation with respect to the microtubule on which it acts but that the N-terminal region rotates around a pivot point and generates a power stroke vector parallel to the coiled-coil stalk. In either scenario, if LC1 indeed tethers the motor unit to the A-tubule, the connection must be disrupted during the power stroke if the γ HC is to function as a motor in situ. Although the purified γ HC–LC1–LC4 complex is competent to act as a microtubule translocase in vitro, it is important to note that in this system, the LC1–microtubule interaction no longer exists (Sakakibara and Nakayama, 1998). Furthermore, we did not observe any apparent nucleotide-dependent alterations in LC1–tubulin complexes. This is consistent with a theoretical consideration (Lindemann and Hunt, 2003) of the data of Burgess et al. (2003), which proposed that binding of a motor unit to the A-tubule might be necessary to provide sufficient rigidity such that a power stroke of 3.8 pN could be generated. In this model, the rigidly tethered γ HC motor might act on the B-tubule in an ATP-dependent manner to limit the amount of sliding between specific doublets rather than acting as microtubule translocase by itself. This suggestion is consistent with the observation that the *oda4-s7* mutant, which lacks only the β HC motor unit, swims at almost the same velocity as strains missing the entire outer arm (Sakakibara et al., 1993) and with one interpretation of the data of Ishikawa et al. (2007), which suggested a fundamentally distinct orientation for the γ HC motor unit in situ compared with the other HCs within the outer arm.

Two possible geometries for the γ HC–LC1–A-tubule ternary complex, which depend on the orientation of the γ HC motor unit, are diagrammed in Fig. 10 d. In one scenario, the motor unit is tethered by one copy of LC1 and motor unit rotation, which would potentially result in release of that copy from the microtubule and binding of the second copy. The alternative model proposes that both LC1 proteins bind the A-tubule simultaneously; in this situation, the γ HC may act as a brake rather than a motor, per se.

In conclusion, we have demonstrated that an LC bound to one outer arm dynein HC tethers this motor unit to a doublet microtubule within the axonemal superstructure and is involved in the control of conformational switching during power/recovery stroke transitions.

Materials and methods

Molecular cloning, tagging, and mutagenesis of the LC1 gene

The LC1 genomic clone was obtained from our wild-type *C. reinhardtii* strain 1132D⁻ genomic DNA library made in λDashII using the previously obtained cDNA (Benashski et al., 1999) as a probe. A 6.2-kb segment containing the entire LC1 gene was excised from the λ insert with XbaI, subcloned into pBluescript II SK−, and sequenced. Subsequently, an oligonucleotide encoding 16 bp of the 5′ untranslated region, the first two LC1 codons, a myc epitope incorporating the *C. reinhardtii* codon bias, a novel HindIII site for screening purposes, and the next eight LC1 codons were synthesized and inserted into the XbaI genomic fragment using standard methods. The following alterations were incorporated into the myc-tagged LC1 gene by site-directed mutagenesis: M182*, M182A, M182G, M182P, D185*, D185G, D185P, R189A, R189E, R196A, and R196D (asterisks indicate stop codons). These specific residues were targeted based on NMR structural and backbone dynamics analyses (Wu et al., 2000, 2003).

Strains and culture conditions

The CC3395 (*cwd arg7-8*) strain of *C. reinhardtii*, which lacks cell walls and is defective in the gene for arginosuccinate lyase, was used as the parental background to express mutant forms of LC1. Stable nuclear cotransformation of the selectable pArg7.8 plasmid and the LC1 gene constructs was achieved using the standard glass bead method after autolysin treatment (Nelson and Lefebvre, 1995). Transformants containing the pArg7.8 plasmid were initially selected by growth on media lacking arginine. Other strains used in this study include cc124, *oda2-t*, *oda4-s7*, *oda4-s7 oda11*, and *oda6*. For motility and biochemical experiments, all strains were grown in R medium bubbled with 5% CO_2/95% air on a 15/9-h light/dark cycle (Witman, 1986).

Molecular analysis of transformants

Transformed strains were screened using the PCR for the insertion of a myc-tagged copy of LC1 containing a novel HindIII restriction site. Subsequently, the presence of myc-LC1 in flagella samples (see Isolation of flagella…) was assessed by immunoblot analysis using the R5932 antibody against LC1 or the 9E10 monoclonal antibody that detects the myc epitope. Southern blot analysis of genomic DNA samples was performed using standard methods (King and Patel-King, 1995).

Isolation of flagella and dynein purification

Flagella were detached from *C. reinhardtii* cell bodies with dibucaine and isolated as described previously (King, 1995). After demembranation with IGEPAL CA-630 (Sigma-Aldrich) in 30 mM Hepes, pH 7.5, 5 mM $MgSO_4$, 0.5 mM EDTA, and 25 mM KCl, dyneins were extracted from the resulting axonemes with 0.6 M NaCl and further purified by density gradient centrifugation in 5–20% sucrose gradients using a rotor (SW55; Beckman Coulter; Takada et al., 1992). Zero-length cross-linking of axonemal samples with EDC in the presence and absence of Ca^{2+}, nucleotides, and/or vanadate was performed as described previously (King et al., 1991; Wakabayashi et al., 2007).

ATPase assays

The ATPase activity of axonemal samples was determined using a phosphate assay system (EnzChek; Invitrogen) that couples phosphate released from ATP to the conversion of 2-amino-6-mercapto-7-methyl-purine riboside to ribose-1-phosphate and 2-amino-6-mercapto-7-methyl-purine. Each assay contained 50 µg axonemes in 30 mM Hepes, pH 7.5, 5 mM $MgSO_4$, 0.5 mM EDTA, and 25 mM K acetate, and the change in absorbance at 360 nm was followed for 5–20 min. A standard curve generated with known amounts of KH_2PO_4 was used to convert change in absorbance to nanomoles of phosphate released per minute per microgram of protein.

Electrophoretic and immunoblot analyses

Samples were routinely separated in 10% acrylamide gels or in 5–15% acrylamide gradient gels containing SDS and either stained with Coomassie blue or blotted to nitrocellulose and stained with 0.1% Reactive brown 10 (aqueous) before immunostaining. Characterization of the R5932 rabbit polyclonal antibody that specifically recognizes LC1 was described previously (Benashski et al., 1999). The myc epitope and tubulin were detected using the 9E10 and B-5-1-2 mouse monoclonal antibodies, respectively. For the blot overlay assay, a nitrocellulose blot was incubated overnight with 0.1% Tween 20 in TBS and then for an additional 1 h with Tween/TBS containing 5% dry milk. The membrane was incubated with Tween/TBS containing 1 mg recombinant LC1, washed extensively, and probed with the R5932 antibody.

Microtubule-binding assay

Recombinant LC1 in 20 mM Hepes, pH 7.5, 5 mM $MgSO_4$, 1 mM EDTA, and 1 mM DTT was first prespun for 5 min in an airfuge at maximum pressure. Bovine brain tubulin (#TL238; Cytoskeleton Inc.) was polymerized with 1 mM GTP in PEM buffer (100 mM Pipes, pH 6.9, 2 mM EGTA, and

1 mM $MgSO_4$) with 1.3 mM DTT and stabilized with 10 µM taxol. Subsequently, LC1 (1.1 mg/ml final concentration) was incubated in the presence or absence of 0.8 mg/ml taxol-stabilized microtubules at room temperature for 30 min. Samples were spun in the airfuge for 5 min. Supernatants and pellets were electrophoresed in 10% acrylamide SDS gels and stained with Coomassie blue. Densitometry was performed using an imaging system (Alpha Innotech).

Analysis of cell swimming behavior

C. reinhardtii flagellar beat frequency was determined as described previously (Wakabayashi and King, 2006) using the population-based fast Fourier transform method of Kamiya (2000), which monitors cell vibration. To determine cell swimming velocity and to track swimming paths, the movement of individual cells was imaged with a video camera (Mintron 7266MD; World Precision Instruments) using a 20×/0.50 UPlan Fluor phase-contrast lens mounted on a microscope (BX51; Olympus); videos were recorded at 15 frames per second using Windows Movie Maker software (Microsoft). Video files were decompiled with Blaze Media Pro (version 7.1; Mystik Media), and cell paths were tracked using MetaMorph software (version 7.0r0; MDS Analytical Technologies). The resulting xy coordinate data were subsequently analyzed, and swimming statistics were calculated with Cell Motility Suite (version1.2; Martens et al., 2006).

For detailed analysis of flagellar waveform, cells were imaged using a camera (X-PRI F1; AOS Technologies) at 600 frames per second using differential interference contrast optics and a 60×/1.40 Plan Apochromat objective on a microscope (BX-51; Olympus). Videos were recorded as 10 bit with an 800 × 560 pixel resolution using Imaging Studio software (version 2.6.0.0; AOS Technologies). Video files were decompiled, and individual frames were assembled into a montage illustrating the waveform. The brightness and contrast were adjusted and the montage processed with the sharpen/unsharpen filters in Photoshop (Adobe) to enhance the visibility of the flagella. The summary diagrams of flagellar waveform were prepared by tracing the flagella outline from sequential frames of the decompiled video onto an acetate sheet, digitizing the drawing, and assembling/aligning the layers in Photoshop.

The response of *C. reinhardtii* swimming behavior to alterations in solution viscosity and calculation of the propulsive force were determined essentially as described previously (Yagi et al., 2005). In brief, Ficoll (type 400; ~400,000 kD molecular mass; Sigma-Aldrich) solutions (0, 1, 3, 5, 8, 12, and 16% wt/vol) were prepared in 10 mM Hepes, pH 7.5, and the viscosity (in centipoise) was determined at 23°C using a calibrated Cannon-Fenske viscometer (size 25; #13-617A; Thermo Fisher Scientific). Strains were resuspended in the Ficoll solutions, and their beat frequency and swimming velocity were determined. Propulsive force was calculated using Stokes equation: $F = 6\pi\eta a v$, where η is the solution viscosity, a is the cell radius, and v is the measured velocity.

Immuno-EM

Axonemes were prepared from the *oda4-s7 oda11* double mutant using standard methods (see above). This strain was chosen, as it lacks the entire α HC and β HC motor domain and thus allows the antibody ready access to the interior portion of the outer arm where the γ HC and its associated components are located. Axonemes were incubated with blot-purified antibody (R5932) against LC1 or with TBS alone for 60 min at room temperature. After buffer washes, samples were incubated for 60 min with goat anti–rabbit IgG secondary antibody conjugated to 5 nm colloidal gold. After additional washes, axoneme pellets were fixed with half-strength Karnovsky's fixative (3% glutaraldehyde and 2% paraformaldehyde) in 0.1 M Na cacodylate, pH 7.2, for 1 h. After a wash with cacodylate buffer, axoneme pellets were postfixed with 1% OsO_4/$KFe(CN)_6$ in cacodylate buffer, stained en bloc with uranyl acetate, dehydrated in ethanol, transitioned to propylene oxide, and embedded in Polybed A12. Sections were stained with 1% uranyl acetate and lead citrate before examination in an electron microscope (CM10; Phillips).

Structure display

The ribbon and van der Waals surface representations of the refined LC1 NMR structure (Protein Data Bank accession no. 1M9L; Wu et al., 2003) were displayed using MOLMOL (Koradi et al., 1996) and PyMOL (DeLano Scientific LLC), respectively.

We thank Ann Cowan (University of Connecticut Health Center, Farmington, CT) for helpful discussions concerning cell tracking using MetaMorph, Masahide Kikkawa (Kyoto University, Kyoto, Japan) for the cryo-EM reconstruction figure, Panteleimon Rompolas for assistance with immuno-EM, and Oksana Gorbatyuk and Sharon Benashski for technical assistance.

This study was supported by grant GM51293 from the National Institutes of Health.

Submitted: 15 May 2009
Accepted: 25 June 2009

References

Baron, D.M., Z.P. Kabututu, and K.L. Hill. 2007. Stuck in reverse: loss of LC1 in *Trypanosoma brucei* disrupts outer dynein arms and leads to reverse flagellar beat and backward movement. *J. Cell Sci.* 120:1513–1520.

Bell, C.W., E. Fronk, and I.R. Gibbons. 1979. Polypeptide subunits of dynein 1 from sea urchin sperm flagella. *J. Supramol. Struct.* 11:311–317.

Belles-Isles, M., C. Chapeau, D. White, and C. Gagnon. 1986. Isolation and characterization of dynein ATPase from bull spermatozoa. *Biochem. J.* 240:863–869.

Benashski, S.E., R.S. Patel-King, and S.M. King. 1999. Light chain 1 from the *Chlamydomonas* outer dynein arm is a leucine-rich repeat protein associated with the motor domain of the γ heavy chain. *Biochemistry.* 38:7253–7264.

Bessen, M., R.B. Fay, and G.B. Witman. 1980. Calcium control of waveform in isolated flagellar axonemes of *Chlamydomonas. J. Cell Biol.* 86:446–455.

Branche, C., L. Kohl, G. Toutirais, J. Buisson, J. Cosson, and P. Bastin. 2006. Conserved and specific functions of axoneme components in trypanosome motility. *J. Cell Sci.* 119:3443–3455.

Brokaw, C.J. 2008. Thinking about flagellar oscillation. *Cell Motil. Cytoskeleton.* doi:10.1002/cm.20313.

Burgess, S.A., M.L. Walker, H. Sakakibara, P.J. Knight, and K. Oiwa. 2003. Dynein structure and power stroke. *Nature.* 421:715–718.

Carter, A.P., J.E. Garbarino, E.M. Wilson-Kubalek, W.E. Shipley, C. Cho, R.A. Milligan, R.D. Vale, and I.R. Gibbons. 2008. Structure and functional role of dynein's microtubule-binding domain. *Science.* 322:1691–1695.

Cho, C., S. Reck-Peterson, and R. Vale. 2008. Cytoplasmic dynein's regulatory ATPase sites affect processivity and force generation. *J. Biol. Chem.* 283:25839–25845.

Freshour, J., R. Yokoyama, and D.R. Mitchell. 2007. *Chlamydomonas* flagellar outer row dynein assembly protein Oda7 interacts with both outer row and I1 inner row dyneins. *J. Biol. Chem.* 282:5404–5412.

Gatti, J.L., S.M. King, A.G. Moss, and G.B. Witman. 1989. Outer arm dynein from trout spermatozoa. Purification, polypeptide composition, and enzymatic properties. *J. Biol. Chem.* 264:11450–11457.

Gatti, J.L., S.M. King, and G.B. Witman. 1991. The ATPases of *Chlamydomonas* outer arm dynein differ in their pH and cationic requirements. *In* Comparative Spermatology 20 Years After. B. Baccetti, editor. Raven Press, New York. 373–375.

Habermacher, G., and W.S. Sale. 1997. Regulation of flagellar dynein by phosphorylation of a 138-kD inner arm dynein intermediate chain. *J. Cell Biol.* 136:167–176.

Hasegawa, E., H. Hayashi, S. Asakura, and R. Kamiya. 1987. Stimulation of in vitro motility of *Chlamydomonas* axonemes by inhibition of cAMP-dependent phosphorylation. *Cell Motil. Cytoskeleton.* 8:302–311.

Hayashi, S., and C. Shingyogi. 2008. Mechanism of flagellar oscillation - bending-induced switching of dynein activity in elastase-treated axonemes of sea urchin sperm. *J. Cell Sci.* 121:2833–2843.

Hayashibe, K., C. Shingyoji, and R. Kamiya. 1997. Induction of temporary beating in paralyzed flagella of *Chlamydomonas* mutants by application of external force. *Cell Motil. Cytoskeleton.* 37:232–239.

Hyams, J.S., and G.G. Borisy. 1978. Isolated flagellar apparatus of *Chlamydomonas*: characterization of forward swimming and alteration of waveform and reversal of motion by calcium ions *in vitro. J. Cell Sci.* 33:235–253.

Ishikawa, T., H. Sakakibara, and K. Oiwa. 2007. The architecture of outer dynein arms *in situ. J. Mol. Biol.* 368:1249–1258.

Kagami, O., and R. Kamiya. 1990. Strikingly low ATPase activities in flagellar axonemes of a *Chlamydomonas* mutant missing outer dynein arms. *Eur. J. Biochem.* 189:441–446.

Kamiya, R. 2000. Analysis of cell vibration for assessing axonemal motility in *Chlamydomonas*. *Methods.* 22:383–387.

Kamiya, R., and M. Okamoto. 1985. A mutant of *Chlamydomonas reinhardtii* that lacks the flagellar outer dynein arm but can swim. *J. Cell Sci.* 74:181–191.

King, S.J., and S.K. Dutcher. 1997. Phosphoregulation of an inner dynein arm complex in *Chlamydomonas reinhardtii* is altered in phototactic mutant strains. *J. Cell Biol.* 136:177–191.

King, S.M. 1995. Large-scale isolation of *Chlamydomonas* flagella. *Methods Cell Biol.* 47:9–12.

King, S.M., and R. Kamiya. 2008. Axonemal dyneins: assembly, structure and force generation. *In* The *Chlamydomonas* Sourcebook: Cell Motility and Behavior, vol. 3. G.B. Witman, editor. Academic Press, San Diego. 131–208.

King, S.M., and R.S. Patel-King. 1995. The $M_{(r)}$ = 8,000 and 11,000 outer arm dynein light chains from *Chlamydomonas* flagella have cytoplasmic homologues. *J. Biol. Chem.* 270:11445–11452.

King, S.M., C.G. Wilkerson, and G.B. Witman. 1991. The M_r 78,000 intermediate chain of *Chlamydomonas* outer arm dynein interacts with α-tubulin *in situ*. *J. Biol. Chem.* 266:8401–8407.

Kon, T., T. Mogami, R. Ohkura, M. Nishiura, and K. Sutoh. 2005. ATP hydrolysis cycle-dependent tail motions in cytoplasmic dynein. *Nat. Struct. Mol. Biol.* 12:513–519.

Koradi, R., M. Billeter, and K. Wuthrich. 1996. MOLMOL: a program for display and analysis of macromolecular structures. *J. Mol. Graph.* 14:51–55.

Lechtreck, K.F., and G.B. Witman. 2007. *Chlamydomonas reinhardtii* hydin is a central pair protein required for flagellar motility. *J. Cell Biol.* 176:473–482.

Lindemann, C.B., and A.J. Hunt. 2003. Does axonemal dynein push, pull, or oscillate? *Cell Motil. Cytoskeleton.* 56:237–244.

Lindemann, C.B., and D.R. Mitchell. 2007. Evidence for axonemal distortion during the flagellar beat of *Chlamydomonas*. *Cell Motil. Cytoskeleton.* 64:580–589.

Lindemann, C.B. 2002. Geometric clutch model version 3: The role of the inner and outer arm dyneins in the ciliary beat. *Cell Motil. Cytoskeleton.* 52:242–254.

Liu, Z., H. Takazaki, Y. Nakazawa, M. Sakato, T. Yagi, T. Yasunaga, S.M. King, and R. Kamiya. 2008. Partially functional outer arm dynein in a novel *Chlamydomonas* mutant expressing a truncated γ heavy chain. *Eukaryot. Cell.* 7:1136–1145.

Martens, L., G. Monsieur, C. Ampe, K. Gevaert, and J. Vandekerckhove. 2006. Cell_motility: a cross-platform, open source application for the study of cell motion paths. *BMC Bioinformatics.* 7:289.

Mitchell, D.R., and J.L. Rosenbaum. 1985. A motile *Chlamydomonas* flagellar mutant that lacks outer dynein arms. *J. Cell Biol.* 100:1228–1234.

Nelson, J.A., and P.A. Lefebvre. 1995. Transformation of *Chlamydomonas reinhardtii*. *Methods Cell Biol.* 47:513–517.

Nicastro, D., C. Schwartz, J. Pierson, R. Gaudette, M.E. Porter, and J.R. McIntosh. 2006. The molecular architecture of axonemes revealed by cryoelectron tomography. *Science.* 313:944–948.

Oda, T., N. Hirokawa, and M. Kikkawa. 2007. Three-dimensional structures of the flagellar dynein-microtubule complex by cryoelectron microscopy. *J. Cell Biol.* 177:243–252.

Pedersen, L.B., P. Rompolas, S.T. Christensen, J.L. Rosenbaum, and S.M. King. 2007. The lissencephaly protein Lis1 is present in motile mammalian cilia and requires outer dynein arm for targeting to *Chlamydomonas* flagella. *J. Cell Sci.* 120:858–867.

Pfister, K.K., R.B. Fay, and G.B. Witman. 1982. Purification and polypeptide composition of dynein ATPases from *Chlamydomonas* flagella. *Cell Motil.* 2:525–547.

Piperno, G., K. Mead, and W. Shestak. 1992. The inner dynein arms I2 interact with a "dynein regulatory complex" in *Chlamydomonas* flagella. *J. Cell Biol.* 118:1455–1463.

Porter, M.E., and K.A. Johnson. 1983. Characterization of the ATP-sensitive binding of *Tetrahymena* 30 S dynein to bovine brain microtubules. *J. Biol. Chem.* 258:6575–6581.

Roberts, A.J., N. Numata, M.L. Walker, Y.S. Kato, B. Malkova, T. Kon, R. Ohkura, F. Arisaka, P.J. Knight, K. Sutoh, and S.A. Burgess. 2009. AAA^+ ring and linker swing mechanism in the dynein motor. *Cell.* 136:485–495.

Sakakibara, H., D.R. Mitchell, and R. Kamiya. 1991. A *Chlamydomonas* outer arm dynein mutant missing the α heavy chain. *J. Cell Biol.* 113:615–622.

Sakakibara, H., and H. Nakayama. 1998. Translocation of microtubules caused by the αβ, β and γ outer arm dynein subparticles of *Chlamydomonas*. *J. Cell Sci.* 111:1155–1164.

Sakakibara, H., S. Takada, S.M. King, G.B. Witman, and R. Kamiya. 1993. A *Chlamydomonas* outer arm dynein mutant with a truncated β heavy chain. *J. Cell Biol.* 122:653–661.

Sakato, M., and S. King. 2003. Calcium regulates ATP-sensitive microtubule binding by *Chlamydomonas* outer arm dynein. *J. Biol. Chem.* 278:43571–43579.

Sakato, M., H. Sakakibara, and S.M. King. 2007. *Chlamydomonas* outer arm dynein alters conformation in response to Ca^{2+}. *Mol. Biol. Cell.* 18:3620–3634.

Salathe, M. 2007. Regulation of mammalian ciliary beating. *Annu. Rev. Physiol.* 69:401–422.

Smith, E.F., and P. Yang. 2004. The radial spokes and central apparatus: mechano-chemical transducers that regulate flagellar motility. *Cell Motil. Cytoskeleton.* 57:8–17.

Sugino, K., and Y. Naitoh. 1982. Simulated cross-bridge patterns corresponding to ciliary beating in *Paramecium*. *Nature.* 295:609–611.

Takada, S., and R. Kamiya. 1994. Functional reconstitution of *Chlamydomonas* outer dynein arms from α- β and γ subunits: requirement of a third factor. *J. Cell Biol.* 126:737–745.

Takada, S., and R. Kamiya. 1997. Beat frequency difference between the two flagella of *Chlamydomonas* depends on the attachment site of outer dynein arms on the outer- doublet microtubules. *Cell Motil. Cytoskeleton.* 36:68–75.

Takada, S., H. Sakakibara, and R. Kamiya. 1992. Three-headed outer arm dynein from *Chlamydomonas* that can functionally combine with outer-arm-missing axonemes. *J. Biochem.* 111:758–762.

Wakabayashi, K., and S.M. King. 2006. Modulation of *Chlamydomonas reinhardtii* flagellar motility by redox poise. *J. Cell Biol.* 173:743–754.

Wakabayashi, K., M. Sakato, and S.M. King. 2007. Protein modification to probe intradynein interactions and in vivo redox state. *In* Methods in Molecular Biology: Molecular Motors. A.O. Sperry, editor. Humana Press Inc., Totowa, NJ. 71–83.

Wickstead, B., and K. Gull. 2007. Dyneins across eukaryotes: a comparative genomic analysis. *Traffic.* 8:1708–1721.

Wirschell, M., G. Pazour, A. Yoda, M. Hirono, R. Kamiya, and G. Witman. 2004. Oda5p, a novel axonemal protein required for assembly of the outer dynein arm and an associated adenylate kinase. *Mol. Biol. Cell.* 15:2729–2741.

Witman, G.B. 1986. Isolation of *Chlamydomonas* flagella and flagellar axonemes. *Methods Enzymol.* 134:280–290.

Wu, H., M. Blackledge, M.W. Maciejewski, G.P. Mullen, and S.M. King. 2003. Relaxation-based structure refinement and backbone molecular dynamics of the dynein motor domain-associated light chain. *Biochemistry.* 42:57–71.

Wu, H., M.W. Maciejewski, S.E. Benashski, G.P. Mullen, and S.M. King. 1999. ^1H, ^{15}N and ^{13}C resonance assignments for the 22 kDa LC1 light chain from *Chlamydomonas* outer arm dynein. *J. Biomol. NMR.* 13:309–310.

Wu, H., M.W. Maciejewski, A. Marintchev, S.E. Benashski, G.P. Mullen, and S.M. King. 2000. Solution structure of a dynein motor domain-associated light chain. *Nat. Struct. Biol.* 7:575–579.

Yagi, T., I. Minoura, A. Fujiwara, R. Saito, T. Yasunaga, M. Hirono, and R. Kamiya. 2005. An axonemal dynein particularly important for flagellar movement at high viscosity: Implications from a new *Chlamydomonas* mutant deficient in the dynein heavy chain gene DHC9. *J. Biol. Chem.* 280:41412–41420.